Simplified generalized-gradient approximation and anharmonicity: Benchmark calculations on molecules

David C. Patton
Complex Systems Theory Branch, Naval Research Laboratory, Washington, D.C. 20375

Dirk V. Porezag
Department of Physics, Chemnitz University of Technology, Chemnitz, Germany

Mark R. Pederson
Complex Systems Theory Branch, Naval Research Laboratory, Washington, D.C. 20375

(Received 29 October 1996)

Recent implementational improvements of the generalized-gradient approximation (GGA) have led to a simplified version which is parametrized entirely from fundamental constants, easier to use, and possibly easier to improve. We have performed detailed calculations on the geometries, atomization energies, vibrational energies, and infrared and Raman spectra of many first- and second-row dimers as well as some polyatomic molecules. For atomization and vibrational energies, we find that the simplified version of GGA leads to results similar to the original version. We comment on the fact that GGA-induced changes of hydrogenic bonding are different than for the other atoms in the periodic table but still an improvement over the local approximations to density-functional theory. In addition to a harmonic treatment of the vibrational modes we include the contributions of anharmonicity as well. With the exception of the light hydrogen containing molecules anharmonic corrections are quite small. [S0163-1829(97)00710-8]

I. INTRODUCTION

In comparison to local-density approximations[1] (LDA's) to the density-functional theory[2] (DFT) the generalized-gradient-approximation[3–5] (GGA) has been shown to improve many properties of materials that are governed by a realistic description of bond formation. In addition to decreasing the total energy of each atom, the generalized-gradient approximation has been shown to remove much of the overbinding that is present in the existing local approximations to DFT. As a result, it is now possible to determine atomization energies to approximately 0.1–0.2 eV/atom[4–6] and to significantly improve the DFT-based determination of reaction barriers.[7–9]

In a recent paper, Perdew, Burke, and Ernzerhof[10] (PBE) present a simplified version of the GGA for density-functional theory. As compared to the earlier version of GGA, the PBE version of GGA improves upon six shortcomings which are discussed in detail in their paper. Despite the simplifications, the authors suggest that the PBE version of GGA should not dramatically alter previous GGA results and present data on the atomization energies of 20 small molecules to illustrate this point. The purpose of this work is to expand upon these results by considering several additional effects and physical characteristics. In addition to performing calculations on a different, albeit partially overlapping, set of molecules some of which exhibit antiferromagnetism, we have included all effects due to geometrical relaxations in the calculation of our atomization energies. Further we have calculated the vibrational modes of all of these molecules as well as the Raman activities and infrared intensities of each of these systems. Finally because of the intrinsic accuracy that is now available with the GGA it is appropriate to include the small effects due to anharmonicity. We have included these effects in our calculations on vibrational transition energies.

II. COMPUTATIONAL DETAILS

To perform the calculations we use the all-electron self-consistent Gaussian-orbital cluster codes of Pederson and Jackson.[11] This method combines large Gaussian-orbital basis sets, numerically precise variational integration techniques, group theory, and the analytic solution of Poisson's equation to accurately determine the self-consistent-field potentials, secular matrix, total energies and Hellmann-Feynman forces. A conjugate-gradient algorithm is used to determine the equilibrium geometries from the Hellmann-Feynman forces. To calculate the vibrational modes we use a forward and backward finite differencing approach.[12] To determine the vibrational spectra we calculate the vibrationally induced changes of the dipole moment and polarizability tensor using the methods discussed in Ref. 13. Since a primary objective of this work is to produce results that are devoid of uncertainties due to basis sets and numerical precision, special care has been taken to achieve fully converged results. For each atom we use a contracted Gaussian-orbital basis set which would exactly reproduce the atomic total energies that would be obtained from a basis set of single Gaussians. In addition we use a total of six even-tempered single Gaussian s- and p-type functions and four even-tempered single Gaussian d-type functions. The contracted atomic basis set is constructed from a set of N even-tempered bare Gaussians with $N=8$ for H, $N=12$ for Li-Ne, $N=15$ for Na-Ar, and $N=18$ for heavier atoms. In addition, for the molecules (Mo, Cr, and Cu) where valence d states may contribute to bond-

TABLE I. Binding energies in eV of a collection of small molecules as calculated within the PW91 LDA, the PW91 GGA, and the PBE GGA. Superscripts designate that the ground-state dimer was magnetic with a multiplicity of 3. Antiferromagnetic ground states are designated with a $\uparrow\downarrow$. Δ is the difference between the calculated and experimental binding energy in eV/atom. At the bottom of the table are listed in eV the average error (δ) and RMS error for each of the approximations.

Molecule	Expt.	LDA	Δ	GGA-PW91	GGA-PBE	Δ
H_2	4.75	4.907	+0.08	4.561	4.540	−0.11
Li_2	1.06	1.031	−0.01	0.912	0.865	−0.10
Be_2	0.11	0.560	+0.23	0.431	0.424	+0.16
$^3B_2$	3.08	3.851	+0.39	3.333	3.345	+0.13
C_2	6.31	7.227	+0.46	6.188	6.229	−0.04
N_2	9.91	11.576	+0.83	10.507	10.539	+0.31
$^3O_2$	5.23	7.621	+1.20	6.283	6.298	+0.53
F_2	1.66	3.441	+0.89	2.433	2.410	+0.38
Ne_2	0.004	0.020	+0.01	0.014	0.006	+0.00
Na_2	0.8	0.885	+0.04	0.796	0.763	−0.02
$^3Al_2$	1.8	1.978	+0.09	1.678	1.676	−0.06
$^3Si_2$	3.1	4.007	+0.45	3.538	3.527	+0.21
P_2	5.08	6.184	+0.55	5.245	5.218	+0.07
$^3S_2$	4.41	5.776	+0.68	4.950	4.944	+0.27
Cl_2	2.51	3.372	+0.43	2.770	2.761	+0.13
Ar_2	0.012	0.029	+0.01	0.010	0.006	+0.00
$^{\uparrow\downarrow}Cr_2$	1.56	3.099	+0.77	1.584	1.520	−0.02
Cu_2	2.03	2.623	+0.30	2.135	2.125	+0.05
$^{\uparrow\downarrow}Mo_2$	4.2	4.782	+0.79	3.846	3.777	−0.21
HF	6.12	7.042	+0.46	6.202	6.176	+0.03
CO	11.23	12.943	+0.86	11.646	11.649	+0.21
BF	7.97	9.116	+0.57	8.136	8.092	+0.06
LiF	6.07	6.753	+0.34	6.055	6.010	−0.03
LiH	2.636	2.638	+0.00	2.362	2.318	−0.16
H_2O	10.17	11.635	+0.49	10.305	10.265	+0.03
CO_2	17.08	20.571	+1.16	18.163	18.158	+0.36
CH_4	18.40	20.059	+0.33	18.297	18.241	−0.03
δ		+0.98		+0.19	+0.17	
RMS		1.27		0.41	0.41	

ing we have included bond-centered functions to further increase the variational freedom of our basis. With respect to numerical precision, the parameters for constructing the variational mesh[11] have been chosen very conservatively. Typically we use 5000 mesh points per atom for first and second row atoms. For transition metals we utilize at least 10 000 mesh points which is enough to numerically evaluate the charge density to $\pm 0.000\,001$.

III. RESULTS

A. Atomization energies

Table I contains the atomization energies for selected small molecules as calculated within PW91 LDA, GGA91 and the most recent (PBE) version of the GGA. For molecules composed of atoms with p-type valence electrons, nonspherical reference atoms have been utilized in the calculation of atomization energies. While the effect of sphericity on total atomic energies is negligible within the LDA,[14] it can be very important in the GGA. For example, the difference between the nonspherical and the spherical oxygen atom is 0.35 eV. As is discussed elsewhere,[16] this energy difference is evidence that improved cancellation of the self-interaction error is obtained with the GGA. Use of only spherical reference atoms may cause serious overestimation of binding energies in GGA calculations. We have treated several molecules with special care. Because Cr and Mo atoms are fully spin polarized in their ground states, Cr_2 and Mo_2 were both studied with the following method. They were placed into antiferromagnetic states at large bondlengths. Then both molecular geometry and spin polarization were allowed to relax until reaching equilibrium. Both molecules were found to retain antiferromagnetic character in their ground states. It is important to note that because no pseudopotential core states are utilized in our calculations complete core-polarization effects are included in the reported results.

For diatomic molecules in which p orbitals account for the bonding, the effect of spin correlation can be important. There are significant energy differences between the paired-spin (singlet) state and the spin (triplet) state containing two unpaired electrons. For dimers with magnetic ground states, we have indicated this in the tables by noting the multiplicity of the molecule as a superscript preceding the molecular symbol. Dimers with antiferromagnetic ground states are designated with a superscript $\uparrow\downarrow$ proceeding them. As Table I shows, both GGA approximations consistently reduce the tendency of the LDA to overbind. Whereas LDA leads to errors in the range of 0.5–1.0 eV/atom, both GGA's produce weak overbinding of about 0.1 eV/atom.

B. Equilibrium bondlengths

In Table II, we present the bondlengths for many light, moderate, and heavy molecules. Neglecting hydrogen-containing molecules we reaffirm that the primary effect of GGA is to increase the bondlengths compared to the LDA bondlength by 0.5–5.0 %. Further, the differences in bondlengths for the two versions of GGA is quite small with the average difference of 1.1% being small compared to the average deviation between LDA and either of the GGA's. In contrast to the molecules that do not contain hydrogen, the hydrogen-containing molecules exhibit the opposite trend. For example, for H_2, the bondlength is decreased from 1.446 (LDA) to 1.415–1.417 for the two GGA's. Examination of the other hydrogen containing molecules (LiH, HF, H_2O, CH_4) shows a similar trend. For these hydrogenic molecules, contraction versus expansion of the bondlength depends on the combined effect of GGA on both the nonhydrogenic valence states as well as the hydrogenic 1s states. For these systems we observe either a slight decrease in bondlength (H_2O, HF, CH_4) or an increase (LiH) that is small compared to the average increase of nonhydrogen containing molecules. For the most part, the GGA and LDA reproduce bondlengths with approximately the same quantitative accuracy with rms deviations from experiment of 0.04 and 0.06 bohr, respectively (excluding Ar_2 and Ne_2).

The empirical trend observed in Table II is that the GGA acts to increase the effective radii of all atoms except hydrogen which shows a reduced effective radius. The reduction in

TABLE II. Equilibrium bondlengths for a collection of small molecules as calculated within the PW91 LDA, PW91 GGA, and PBE GGA. Excluding Ne_2 and Ar_2, the RMS deviation from experiment is 0.06, 0.04, and 0.04 bohr, respectively, for the three theories. The average deviation is -0.02, $+0.03$, and $+0.03$ bohr respectively, showing that GGA has a greater tendency to overestimate bondlengths than LDA.

Molecule		Expt.	LDA	GGA-PW91	GGA-PBE
H_2		1.401	1.446	1.415	1.417
Li_2		5.051	5.125	5.165	5.161
Be_2		4.65	4.522	4.608	4.594
$^3B_2$		3.04	3.057	3.060	3.061
C_2		2.348	2.353	2.367	2.370
N_2		2.074	2.069	2.082	2.083
$^3O_2$		2.282	2.278	2.306	2.306
F_2		2.668	2.626	2.675	2.675
Ne_2		5.839	4.790	5.585	5.866
Na_2		5.82	5.672	5.839	5.834
$^3Al_2$		4.66	4.651	4.703	4.703
$^3Si_2$		4.24	4.291	4.322	4.320
P_2		3.578	3.581	3.607	3.606
$^3S_2$		3.570	3.591	3.624	3.620
Cl_2		3.755	3.769	3.821	3.818
Ar_2		7.10	6.369	6.741	7.336
$^{\uparrow\downarrow}Cr_2$		3.17	2.989	3.231	3.226
Cu_2		4.20	4.116	4.237	4.257
$^{\uparrow\downarrow}Mo_2$		3.65	3.589	3.684	3.622
HF		1.733	1.759	1.754	1.756
CO		2.132	2.130	2.144	2.147
BF		2.38	2.377	2.403	2.406
LiF			2.917	2.955	2.959
LiH			3.031	3.026	3.032
H_2O	R_{OH}	1.809	1.833	1.829	1.830
	θ_{HOH}	104.5	104.96	104.35	104.23
CO_2	R_{CO}	2.192	2.197	2.211	2.213
CH_4	R_{CH}	2.050	2.074	2.068	2.071

H bondlengths can be directly attributed to the GGA influence on 1*s*-core electrons. We have looked at the amount of 1*s*-core charge enclosed within a sphere of radius $1/Z$ (Z=nuclear charge) for several atoms and in all cases we find that GGA causes 1*s*-core charge to flow into this sphere. By transferring charge from the tail of a 1*s*-core state inward toward the nucleus the resulting GGA density decays a bit faster than the corresponding LDA density which should be energetically preferred. Since the GGA prefers more compact 1*s*-core states it is natural to expect that hydrogen bonds will show a tendency to decrease or to oppose the uniform bondlength expansion that is observed for all other atoms. The tendency toward more compact core states within GGA should also play a role in *increasing* the bondlengths of most molecules since the more compact core states lead to a more effective screening of the nuclear coulomb potential. This entices the valence wave functions to expand.

In addition to the well-bound molecules we include results for Ne_2 and Ar_2 as well. While it is clear that GGA, LDA, or any mean-field theory is incapable of accounting for a long-range fluctuating dipole attraction of a van der Waals (VDW) system, we are unaware of a proof that other short-range interactions could not dominate the VDW binding at short range. A critical point for calculations on weakly bound systems is to ensure that basis-set superposition errors (BSSE) cannot be the cause of a weak binding. For Ar_2 and Ne_2 we have performed the requisite calculations to exclude the possibility of BSSE. This involves calculating the atomic total energy with the basis from the dimer calculation at the position of the optimized geometry of the dimer. For example, within the GGA-PBE our calculations of the argon dimer contain BSSE of less than 0.001 eV. For Ar_2, the three mean-field approximations predict a bound state with equilibrium separations of 6.369, 6.741, and 7.336 bohrs, respectively. All of these separations are in good agreement with the experimental value of 7.10 bohrs. The Ne_2 bondlength differs by less than 5% of the experimental value within the GGA. We are certain that there are no numerical uncertainties which would change the qualitative results for these two weakly bound molecules.[15]

C. Harmonic vibrational energies

In Table III, we compare the vibrational modes calculated within the three approximations to experiment. In previous calculations,[16] a softening of most vibrational modes has been observed. We reaffirm this trend for the newer form of the GGA. Excluding beryllium, deviations between the two GGA's are negligible and the average deviation from the experimental frequencies are 4% for the LDA and 3% for the two nonlocal approximations. Because of the contraction of hydrogen bonds by the two GGA's there is an associated hardening of these bonds. This leads to an increase in harmonic vibrational frequencies calculated by the two GGA's as compared to the LDA result for the hydrogen dimer. In systems containing bonding between hydrogen and other species, GGA does not always soften vibrational modes and may in some cases (H_2O, CH_4) produce higher frequencies than the LDA. These increases lead to closer agreement with experiment in the hydrogenic molecules examined in this study.

D. IR and Raman spectra, anharmonicity

As the approximations to the DFT attain greater accuracy more stringent tests are required to assess the capabilities of density-functional theory. In the past it has been quite common to assess the relative merits of energy functionals by comparing energies, geometries and, to some extent, frequencies and polarizabilities to experimentally observable values. These quantities depend most critically on the functional and the first and second derivatives of the functional. One possible means for further assessing the merits of DFT is to compare the infrared and Raman spectra of molecules to experiment since these quantities depend on the second- and third-order derivatives of the energy with respect to applied field and atomic displacements. Alternatively, the ability to simulate optically observable vibrational spectra within the density-functional allows for a new level of interaction between theoretical and experimental materials physics since comparisons between theory and experiment allow an indirect means for deducing geometrical information and for determining the location of isotopes in molecules. To deter-

TABLE III. Harmonic vibrational frequencies in cm^{-1} as calculated within the PW91 LDA, PW91 GGA, and PBE GGA. The average absolute deviation from the experimental value is 61, 47, and 49 cm^{-1}, respectively, for the three theories. The RMS values of 81, 59, and 62 cm^{-1} clearly show that the GGA predicts harmonic frequencies with greater accuracy than the LDA.

Molecule		Expt.	LDA	GGA-PW91	GGA-PBE
H_2		4400	4188	4332	4323
Li_2		351	337	334	333
Be_2		294	371	347	348
$^3B_2$		1051	1014	1011	1017
N_2		2358	2405	2357	2358
$^3O_2$		1580	1612	1543	1547
F_2		917	1063	998	1003
Ne_2			81	44	36
Na_2		160	164	156	157
$^3Al_2$		350	349	341	341
$^3Si_2$		510	492	483	486
P_2		780	786	771	773
$^3S_2$		730	700	700	695
Cl_2		560	548	523	522
Ar_2			62	58	27
$^{\uparrow\downarrow}Cr_2$		470	580	379	390
Cu_2		265	283	261	261
HF		4139	4004	4003	4001
CO		2170	2181	2135	2131
BF			1418	1372	1367
LiF			945	910	915
LiH			1378	1378	1380
H_2O	$1A_1$	1648	1545	1590	1590
	$2A_1$	3832	3722	3721	3714
	$1B_2$	3943	3831	3825	3818
CO_2		667	648	639	637
		1388	1354	1323	1323
		2349	2414	2348	2352
CH_4	$1T_2$	1357	1250	1292	1286
	$1E$	1567	1480	1515	1510
	$1A_1$	3037	2957	2973	2968
	$2T_2$	3158	3085	3086	3081

mine the infrared and Raman response of these small molecules to applied electric fields we have utilized the approach which has been described recently[13] and shown to yield results of reasonable accuracy for hydrocarbon molecules. Since Raman and IR spectra correspond to observable rather than harmonic excitations we have included the effects of anharmonicity as well. Before discussing the results we briefly explain our procedure for doing this.

For each of the molecules we have performed a series of total energy and force evaluations as a function of eight different displacements from the PBE equilibrium geometry. The displacements range from ± 0.02 to ± 0.30 bohr from equilibrium. We use the conjugate-gradient method to perform a least-squares fit of the energies and forces to a polynomial of degree four and then solve the one-dimensional anharmonic Schroedinger equation using a basis of the lowest 15 harmonic eigenfunctions. The lowest excitation energy is then simply determined by taking the difference between the two lowest eigenvalues. We have ascertained that this method is weakly dependent on basis-set size. The same answers are obtained when we use only the five lowest harmonic eigenfunctions as a basis. In Fig. 1 we show a picture of the PBE potential for the O_2 dimer and the two lowest eigenfunctions obtained in this manner.

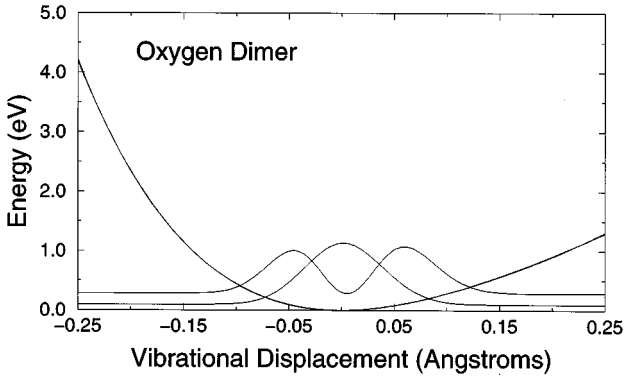

FIG. 1. Pictured above is the potential energy curve for the triplet state of the O_2 molecule as calculated within the PBE GGA energy functional. Also pictured are the densities of the two lowest anharmonic vibrational wave functions which, for presentational purposes have been shifted upward by their eigenvalues. Superimposed on the graph is our fourth-order polynomial fit of the potential energy obtained from the energies and forces. Within the PBE GGA the triplet state of the O_2 dimer is bound by 6.298 eV.

In Table IV we present the absolute IR intensities, I^{IR} and relative Raman activities I_{Raman} as calculated within the GGA-PBE along with the associated harmonic frequencies. Because homonuclear dimers are not IR active by symmetry the value of their IR intensity is exactly zero. We also provide the associated anharmonic frequencies for selected molecules. Since potential-energy curves are similar on the scale of differences in masses of atoms, the largest anharmonic effects are obtained for molecules containing hydrogen. For example, for H_2 we obtain a lowest excitation energy of 4152 cm^{-1} which is in excellent agreement with the observed anharmonic excitation energy of 4161 cm^{-1}.[17] Our anharmonic constants are 116 cm^{-1} for $\omega_e\chi_e$ and 25.5 cm^{-1} for $\omega_e y_e$. For N_2, agreement with experiment is again excellent with the experimental value of the excitation energy being 2330 cm^{-1} (Ref. 18) compared with our calculated value of 2325 cm^{-1}. Since in the case of N_2 our harmonic vibrational energy ω_e is equivalent to the observed value, the small discrepancy in the anharmonic excitation energy comes from higher terms in the expansion.[19] Our value of 13.8 cm^{-1} for $\omega_e\chi_e$ is comparable to the observed value of 14.1 cm^{-1}.[18] We also have a calculated value of 0.4 cm^{-1} for $\omega_e y_e$. Our values of the anharmonic excitation energies for O_2 and CO are in reasonable agreement with the observed values of 1556 and 2143 cm^{-1},[18] respectively. Our anharmonic constants, $\omega_e\chi_e$ and $\omega_e y_e$, are 10.7 and 0.6 cm^{-1} for O_2 and are 12.3 and 0.3 cm^{-1} for CO. These are in excellent agreement with the observed $\omega_e\chi_e$ values of 12.0 and 13.3 cm^{-1} (Ref. 18) for O_2 and CO, respectively. The observed value of $\omega_e y_e$ for O_2 is 0.05 cm^{-1}.

From the results discussed in the preceding paragraph, it appears that the deviation of our calculated values for the anharmonic excitation energy from experiment is solely due

TABLE IV. Vibrational absorptions, IR intensities in Debye/(Å^2)/amu and total Raman scattering activity in Å^4/amu as calculated within the PBE GGA functional. Frequencies marked with a superscript *a* include anharmonic corrections and correspond to the lowest dipole allowed vibrational excitation (e.g., nominally $n=1/2$ to 3/2).

Molecule	ΔR_e	ω_e	I^{IR}	I_{Raman}
H_2	0.049	4152[a]	0.0000	1161.4725
Li_2	0.044	330[a]	0.0000	1993.7640
Be_2		349[a]	0.0000	15.0663
$^3B_2$	0.010	1003[a]	0.0000	452.7844
N_2	0.007	2325[a]	0.0000	21.4143
$^3O_2$	0.009	1523[a]	0.0000	14.3326
$^3F_2$	0.010	1003	0.0000	6.6448
Ne_2		36	0.0000	0.0026
Na_2	0.018	157	0.0000	1351.1771
$^3Al_2$	0.013	334[a]	0.0000	3260.5878
$^3Si_2$	0.008	475[a]	0.0000	2273.8652
P_2	0.002	773[a]	0.0000	61.5369
$^3S_2$	0.002	684[a]	0.0000	37.2997
Cl_2	0.007	516[a]	0.0000	12.6525
Ar_2		27	0.0000	0.0095
$^{\uparrow\downarrow}Cr_2$		390	0.0000	36.6362
Cu_2		261	0.0000	39.4308
HF	0.000	4006[a]	1.6617	30.8194
CO	0.008	2100[a]	1.3383	12.2404
BF	0.011	1341[a]	3.0875	4.6820
LiF	0.022	907[a]	2.7787	14.8830
LiH	0.047	1380	3.1250	834.9284
H_2O	$1A_1$	1590	1.5882	0.8994
	$2A_1$	3714	0.0364	93.0892
	$1B_2$	3818	1.2360	24.7488
CO_2		637	0.4983	0.0238
		1323	0.0000	26.0450
		2352	12.7015	56.9220
CH_4	$1T_2$	1286	0.2995	0.5011
	$1E$	1510	0.0000	2.6236
	$1A_1$	2968	0.0000	226.8640
	$2T_2$	3081	0.4419	46.0390

to the deviation between the calculated harmonic frequency and the observed harmonic frequency. While some experimental information is lacking, we note that for most molecules the effect on the lowest anharmonic excitation is quite small. Also included in Table IV are the anharmonic corrections to the molecular bondlength which is determined from the expectation value of the radius of the anharmonic wave function. As expected, the bondlength increases in all cases with the largest shift of 0.04 bohr in the case of the H_2 molecule.

IV. CONCLUSIONS

To summarize we have determined the atomization energies, bondlengths, and vibrational energies for many different molecules within the LDA, GGA91, and GGA-PBE approximations to density-functional theory. The results presented here include all effects due to self-consistency and have been performed with extremely large well-converged basis sets. These results should provide excellent benchmarks for development of pseudopotentials or for future spectral calculations.

The same improvements that were observed in the GGA91 are attained in the simplified PBE GGA and, as expected from Ref. 10, no remarkable difference in results is observed. We have discussed the fact that hydrogen bonds deviate from the expected lengthening of bonds and softening of vibrational modes. This result is explained by noting that the GGA becomes more stable as density gradients increase. Since the H-core state can increase the density-gradient by transferring charge from the tail of the atom to the nucleus, the size of a hydrogen atom decreases which often leads to a *shortening* of the hydrogen bonds. The reduction of hydrogen bonds also impacts vibrational spectra of such systems. Rather than a uniform softening of such bonds there is a stronger tendency toward hardening. We further suggest that the reduction of 1*s*-core wave functions in other atoms leads to a core Coulomb potential that is more repulsive. This reinforces expectations toward bond lengthening in other systems, since the GGA valence states react to minimize the Coulomb repulsion and therefore have a greater tendency to avoid the core region.

In addition to determining harmonic vibrational frequencies we have gone beyond this approximation and determined the experimentally observable vibrational energies as well as their Raman and IR intensities. The PBE-GGA anharmonic vibrational energies are in excellent agreement with available experimental data which suggests that the use of DFT for the determination of a materials vibrational spectra should be a useful tool for future investigations.

ACKNOWLEDGMENTS

We thank Dr. J.P. Perdew, Dr. K. Burke, and Dr. M. Ernzerhof for providing us with subroutines for their simplified GGA method. Work was supported in part by the ONR Georgia Tech Molecular Design Institute (N00014-96-1-1116), the NSF/DAAD INT-9514714. D.C.P. acknowledges the support of the National Research Council. M.R.P. acknowledges computational support from the Department of Defense High Performance Computing Centers.

[1] See, for example, J. P. Perdew and A. Zunger, Phys. Rev. B **23**, 5048 (1981); R. O. Jones and O. Gunnarsson, Rev. Mod. Phys. **61**, 689 (1989), and references therein.

[2] P. Hohenberg and W. Kohn, Phys. Rev. B **136**, 864 (1964); W. Kohn and L. J. Sham, Phys. Rev **140**, A1133 (1965).

[3] D. C. Langreth and J. P. Perdew, Phys. Rev. B **21**, 4569 (1980); D. C. Langreth and M. J. Mehl, *ibid.* **28**, 1809 (1983); C.D. Hu and D. C. Langreth, Phys. Scr. **32**, 391 (1985); J. P. Perdew,

Phys. Rev. Lett. **55**, 1665 (1985); J. P. Perdew and Y. Wang, Phys. Rev. B **33**, 8800 (1986); A. D. Becke, Phys. Rev. A **38**, 3098 (1988).

[4] J. P. Perdew, J. A. Chevary, S. H. Vosko, K. A. Jackson, M. R. Pederson, D. J. Singh, and C. Fiolhais, Phys. Rev. B **46**, 6671 (1992); **48**, 4979 (E) (1993).

[5] A. D. Becke, J. Chem. Phys. **96**, 2155 (1992).

[6] E. I. Proynov, E. Ruiz, A. Vela, and D. R. Salahub, Int. J. Quantum Chem. S **29**, 61 (1995).

[7] T. Ziegler and L. Fan, J. Am. Chem. Soc. **114**, 10 890 (1992); L. Deng, T. Ziegler, and L. Fan, J. Chem. Phys. **99**, 3823 (1993).

[8] B. Hammer, K. W. Jacobsen, and J. K. Norskov, Phys. Rev. Lett. **70**, 3971 (1993); B. Hammer and M. Scheffler, *ibid.* **74**, 3487 (1995).

[9] M. R. Pederson, Chem. Phys. Lett. **230**, 54 (1994); M. R. Pederson and D. Porezag, J. Phys. Chem. **102**, 9349 (1995).

[10] J. P. Perdew, K. Burke, and M. Ernzerhof, Phys. Rev. Lett. **77**, 3865 (1996).

[11] M. R. Pederson and K. A. Jackson, Phys. Rev. B **41**, 7453 (1990); K. A. Jackson and M. R. Pederson, *ibid.* **42**, 3276 (1990); M. R. Pederson and K. A. Jackson, *ibid.* **43**, 7312 (1991); M. R. Pederson and K. A. Jackson, in *Density Functional Methods in Chemistry*, edited by J. K. Labanowski and J. W. Andzelm (Springer-Verlag, Berlin, 1991).

[12] A. A. Quong, M. R. Pederson, and J. L. Feldman, Solid State Commun. **87**, 535 (1993).

[13] D. V. Porezag and M. R. Pederson, Phys. Rev. B **54**, 7830 (1996).

[14] J. F. Janak and A. R. Williams, Phys. Rev. B **12**, 6301 (1981).

[15] For Ar_2 and PBE GGA, we have checked the results in the table with great detail. We have used a basis set of 18 *optimized* Gaussians which range between 168 179 1 and 0.0942 and have been fully optimized for density-functional calculations. A total of 93 basis functions were placed on each atom. As a test of the numerical integration mesh we note that both the charge and kinetic energy were integrated to 11 decimal places. The kinetic energy was converged to 10^{-8} Hartree. All possible sources of basis set and mesh superposition errors were accounted for and were found to be small compared to the binding energy presented in Table I.

[16] F. W. Kutzler and G. S. Painter, Phys. Rev. B **45**, 3236 (1992).

[17] P. J. Brannon, C. H. Church, and C. W. Peters, J. Mol. Spectrosc. **27**, 44 (1968); B. P. Stoicheff, Can. J. Phys. **35**, 730 (1967).

[18] V. H. Schuler and K. L. Wolf, Z. Phys. **34**, 343 (1925); L. J. F. Hermans, J. J. de Groot, M. F. P. Knaap, and J. J. M. Beenakker, Physica **31**, 1567 (1965).

[19] While we have included the $n=1/2$ to $n=3/2$ transition for predicting the actual observed transition frequency, we note that at higher temperatures experiments also see higher transitions which would have different anharmonic effects.